Available online at www.sciencedirect.com
ScienceDirect
Ceramics International 37 (2011) 1865–1871
CERAMICS INTERNATIONAL
www.elsevier.com/locate/ceramint

Sintering kinetics of a $18.8Li_2O$ $8.3ZrO_2$ $64.2SiO_2$ $8.7Al_2O_3$ glass ceramic

Oscar Rubem Klegues Montedo *, Fernando Joaquim Floriano, Jaime de Oliveira Filho

Unidade Acadêmica de Ciências, Engenharias e Tecnologia (UNACET), Universidade do Extremo Sul Catarinense (UNESC), 88806-000 Criciúma, SC, Brazil
Cynthia Morais Gomes, BAM Federal Institute for Materials Research and Testing, Department of Materials Engineering, 12205 Berlin, Germany*
Dachamir Hotza, Antonio Pedro Novaes de Oliveira, Department of Mechanical Engineering (EMC), Group of Ceramic and Glass Materials (CERMAT), Federal University of Santa Catarina (UFSC), 88040-900 Florianópolis, SC, Brazil

Received 11 November 2010; received in revised form 26 November 2010; accepted 7 February 2011
Available online 8 April 2011

Abstract

The LZSA (Li_2O-ZrO_2-SiO_2-Al_2O_3) glass ceramic system has shown high potential as low temperature co-fired ceramics, the so called LTCC, for several applications, such as screen-printed electronic components, due to its low sintering temperature (< 1000 °C). However, a good microstructural control must be achieved in order to obtain a low porosity material. The $18.8Li_2O$ $8.3ZrO_2$ $64.2SiO_2$ $8.7Al_2O_3$ LZSA glass ceramic composition was prepared by melting, quenching in water, and grinding in order to obtain a very fine powder (3.78 μm mean particle size). Subsequently, compacted bodies were obtained by uniaxial pressing (40 MPa) and drying. Sintering kinetics was investigated by optical dilatometry measurements and scanning electron microscopy (SEM) observations. The activation energy for sintering was found to be 314 $kJ.mol^{-1}$, whilst a maximum linear shrinkage of 22% and porosity of 3.5% were obtained with 10 min swelling time at 800 °C.

Keywords: Ceramics; Glass; Glass ceramics; LZSA; Sintering; Kinetics

1. Introduction

The LZSA (Li_2O-ZrO_2-SiO_2-Al_2O_3) glass ceramic system has been investigated since 2001 [1] due to its interesting chemical, mechanical, thermal, and electrical properties. In fact, Montedo et al. [2] have demonstrated that LZSA glass ceramics based on β-spodumene$_{(ss)}$ ($Li_2O{\cdot}Al_2O_3{\cdot}$4-10$SiO_2$) and zircon ($ZrSiO_4$) crystalline phases have shown good chemical resistance (maximum weight loss of 0.005% in acid solution and 0.01% in basic solution, according to ISO/R 719), high bending strength as well as high abrasion resistance (110 MPa 3-point bending and 95 mm^3, respectively) when compared with traditional ceramic materials, a coefficient of thermal expansion (CTE) ranging from 4.6 to 9.1x10^{-6} $°C^{-1}$ (25 to 325 °C). Additionally to this, Gomes et al. [3] have found a dielectric constant (1 MHz at room temperature) of 8.61 ± 0.84 for laminated bodies crystallized at 850 °C/30 min. Previous results obtained by Montedo et al. [4] at non-optimized sintering conditions showed that a denser material was not obtained because of the crystallization that reduced the thermal shrinkage rate during continuous heat-treatment.

Sintering of powdered glasses by viscous flow proposed by Frenkel [5] was successfully studied by a big amount of researchers, such as Kingery and Berg [6], Scherer [7], and Kim and Khalil [8], among many others. In all cases, sintering is supposed to occur before crystallization. Accordingly, a viscous liquid phase appears during the first stage of sintering, whilst viscous flow sintering with simultaneous crystallization should happen in the next stage of the sintering process of LZSA glass ceramics. This is the reason why sintering control (temperature, time, composition of the parent glass, viscosity of the glassy phase, etc.) is essential for the achievement of a highly dense material.

Dilatometry measurements were carried out to describe the kinetics of the initial-stage sintering by means of the constant rate of heating (CRH) technique, as exposed by Woolfrey and Bannister [9]. According to Cutler [10], yielding low data scatter is a convenient technique to describe the activation energy in respect of the series of isothermal experiments.

From the general equation for isothermal initial stage sintering, Young et al. [11] derived equations for shrinkage and

* Corresponding author. Tel.: +55 48 30454705; fax: +55 48 34312750.
E-mail address: oscar.rkm@gmail.com (O.R.K. Montedo).

0272-8842/$36.00
doi:10.1016/j.ceramint.2011.03.047

shrinkage rates as a function of temperature for two spheres. According to t o Woolfrey and Bannister [9], both of them may be used for data analysis, however the shrinkage plot ($\ln(\Delta l/l_o)$ *vs.* $1/T$) is simpler and generates less data scatter. Here, $\Delta l/l_o$ is the fractional linear shrinkage (%) and T is temperature (K). The plot of $\ln(\Delta l/l_o)$ *vs.* $1/T$ gives a straight line with a slope very near to $-Q/(n+1)R$, if there will be no change in the rate-controlling mechanism of sintering, where Q is the energy activation, n is a constant depend on the rate-controlling mechanism and the particle geometry, and R is the gas constant.

Moreover, the Dorn method was also successfully used to determine the activation energy by Cutler [10], of which a synthetic description was given by Bacmann and Cizeron [12]. According to their method, an instantaneous raise in temperature, ΔT, of the order of 20 °C, followed by shrinkage measurement at that new temperature, can be used to evaluate the apparent activation energy of the process responsible for sintering as given by Eq. 1:

$$Q \cong [RT_1T_2/(T_1 - T_2)]\ln(V_1/V_2) \quad (1)$$

where V_1 is the shrinkage rate at temperature T_1 (K) just before the temperature change, V_2 is the shrinkage rate at T_2 (K) just after the change, and R is the gas constant.

However, according to Khalil and Boccaccini [13] above the crystallization temperature the amorphous phase content is markedly reduced and the crystalline phase formed becomes a barrier for the viscous flow. As a consequence, the effective viscosity of the system increases, although the viscosity of the residual glassy phase decreases with increasing temperature. As a result, relative density values above 95% were not obtained in the LZSA glass ceramic system. On the other hand, it is known that porosity deteriorates several material properties, including electrical, thermal, and mechanical properties, according to Rice [14]. Specifically, Boccaccini and Fan [15] demonstrated that the pore structure (distribution, shape, and orientation) affects the properties of the porous bodies. In this context, a sintering kinetics study was carried out to determine the optimum sintering conditions for achieving a high- density, low-porosity material. Combined techniques were used to obtain a LZSA glass ceramic with adequate properties for LTCC of gradient structures for microelectronics.

2. Material and methods

A $18.8Li_2O$ $8.3ZrO_2$ $64.2SiO_2$ $8.7Al_2O_3$ glass ceramic composition was prepared from appropriate amounts of Li_2CO_3, $ZrSiO_4$, SiO_2, and spodumene ($LiAl[Si_2O_6]$) as raw materials (Colorminas Colorifício e Mineração, Criciúma, Brazil). About 1 kg of a homogeneous frit was obtained after melting of raw materials at 1550 ± 3 °C for 2 h in a gas furnace using a mullite crucible. A small amount of the melt was poured into a graphite crucible, transferred to a Linn High Therm LM 421.27 1300 °C annealing furnace (Linn High Therm, Eschenfelden, Germany) and held at 570 °C for 1 h to obtain small monoliths (50 mm x 5 mm x 4 mm) that were used to determine the glass transition temperature (T_g) in the beam-bending test (Beam-Bending Viscosimeter Bähr Thermoanalyse VIS 401, Hüllhorst, *Germany*) at 10 °C.min^{-1}. The obtained frit was dried and dry-milled in a porcelain ball mill for 3 h and then sieved to yield a powder. The mean particle size of the glass powder was determined by using a laser scattering particle size analyzer (Cilas 1064L particle size analyzer, Orleans, France). The onset of the crystallization peak was determined in a high-temperature thermoanalyzer (STA 409 EP, Netzsch, Selb, Germany; 5°C.min^{-1} heating rate, dry air), using an empty alumina crucible as reference material. Subsequently, the powdered glass was processed by uniaxial pressing in a hydraulic press at 40 MPa (1.40 ± 0.04 g.cm^{-3} green density) in a steel die (75 mm length, 25 mm width, and 5 mm height). The obtained green compacts were then subjected to optical dilatometry measurements (Misura® HSM ODHT 1400, Modena, Italy; 5 °C.min^{-1} heating rate, air) so that linear shrinkage ($\Delta l/l_o$) was evaluated. Two heating programs were applied for the sintering, with and without swelling time. In both cases, the samples were continuously heated up to melting. The sintering temperatures were 685, 800, 900, and 1020 °C, respectively. For each sintering temperature, a 60 min holding time was applied, except for the last one (180 min). After sintering, each sample was cooled down to room temperature. Relative densities were calculated taking into account the ratio between apparent and theoretical densities of the heat treated samples. Theoretical densities of the glass powder and the glass ceramics were measured by He pycnometry (AccuPyc 1330, Micromeritics, Norcross, GA; 5 measurements), whilst apparent geometric densities of the compacted bodies (40 MPa, 1.4 g.cm^{-3} green density) were measured by means of dimensional measurements. For microstructure characterisation, each sample was transversally cut, ground and polished with 1 μm alumina paste and then etched in 2% HF for 25 s. All polished and etched samples were coated with a thin Au film for scanning electron microscopy (SEM) observations (Philips XL 30, Eindhoven, The Netherlands).

3. Results and discussion

3.1. General

The obtainment of porous-free final products based on glass ceramics needs a controlled crystallization and sintering reaction.

The powdered glass used in this work showed low mean particle size (d_{50} = 3.78 μm) and a high specific surface area (Fig. 1). All particles are below 25 μm in size. This is to say that an induction of surface crystallization and a prevention of the densification progress can be expected for this glass. In fact, according to Shyu and Lee [16], the crystallization on the surface of the glass particles raises the glass viscosity inhibiting the sintering by viscous flow. In this case, a suitable heat-treatment (temperature *vs.* time) preferably before the start of crystallization should be carried out to achieve high levels of densification. This implies that a suitable temperature for sintering must be defined.

Fig. 2 shows the viscosity of the glass determined in the beam-bending test. From Fig. 2, the glass temperature

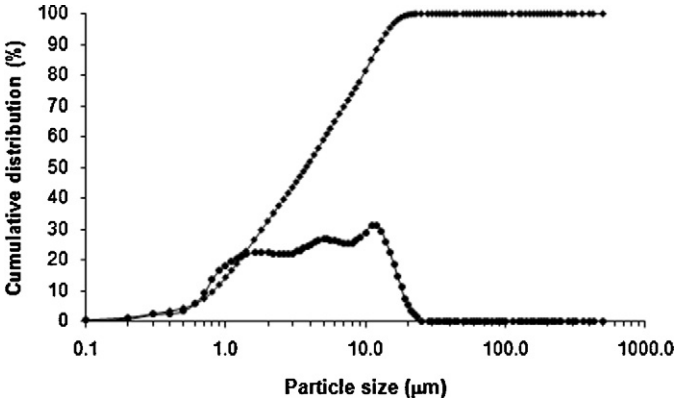

Fig. 1. Particle size distribution of the investigated glass parent.

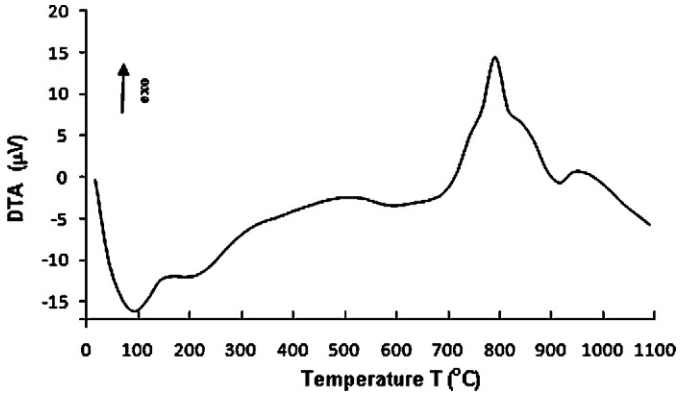

Fig. 3. DTA plot of the investigated composition.

transition T_g at a viscosity of $10^{13.3}$ dPa.s that provides the starting temperature of sintering can be identified [8]. The temperature of 580 °C is in good agreement with the T_g provided by DTA scan (Fig. 3).

Fig. 3 shows the DTA scan of the investigated glass. The first onset of crystallization (T_{c1}) was found to occur at 790 °C, but crystallization can be anticipated to start before 700 °C. The temperature interval for sintering, T_c - T_g, can be considered relatively narrow in this case, i.e. around 200 °C. Moreover, Fig. 3 shows a not well defined crystallization peak at about 850 °C, T_{c2}, related to the zircon ($ZrSiO_4$) crystalline phase. The crystallization rate tends to move down to zero at circa 900 °C.

3.2. Identification of the crystalline phases

Crystalline phases formed during heating are illustrated in Fig. 4 showing XRD patterns recorded of samples after heat treatment for 10 min at the specified temperatures. Solid solutions of β-spodumene (β-spodumene$_{ss}$, $Li_{0\text{-}6}Al_{0\text{-}6}Si_{2\text{-}4}O_6$, ICCD card No. 21-503; $LiAlSi_3O_8$, ICCD card No. 15-27), zircon ($ZrSiO_4$, ICCD card No. 6-266) were identified as the main crystalline phases formed. The material was essentially vitreous at room temperature except for the traces of zirconia (monoclinic ZrO_2, *m*-ZrO_2, ICCD card No. 13-307). Taking into account the relative heights of the peaks, it can be observed that:

a) The β-spodumene$_{ss}$ starts to crystallize at around 670 °C and achieves the maximum peak height at about 800 °C, which is in good agreement with T_{c1}. There is no significant change in the main peak of this crystalline phase from 800 °C;
b) The $ZrSiO_4$ crystallizes in the temperature range between 775 and 900 °C. The maximum peak height is achieved at about 850 °C and can be related to T_{c2};
c) The low-intensity peaks related to the *m*-ZrO_2 crystalline phase at room temperature were detected due to a devitrification occurred during the quenching process. However, the relative peak height of *m*-ZrO_2 became lower from 825 °C probably due to a reaction with silicon oxide (SiO_2) present in the parent glass to form $ZrSiO_4$, since the relative peak height of $ZrSiO_4$ increasingly grows from 800 °C to 850 °C.

3.3. Crystallization mechanism

Although sintering is supposed to be a thermally activated process, when crystallization starts, sintering rates markedly decrease for this glass ceramic system. In fact, this behavior can be associated with the crystallization mechanism since LZSA glass ceramics presents surface crystallization as demonstrated

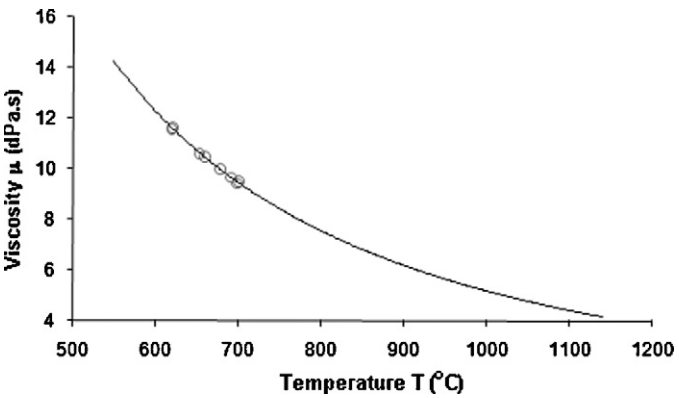

Fig. 2. Plot of the glass viscosity *vs.* temperature by beam-bending test.

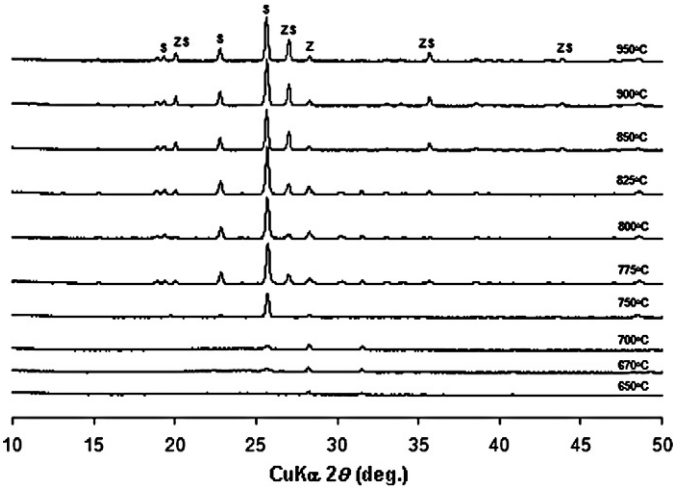

Fig. 4. XRD patterns recorded of the samples after heat treatment for 10 min in the specified temperatures: S: β-spodumene$_{ss}$; ZS: $ZrSiO_4$; Z: ZrO_2.

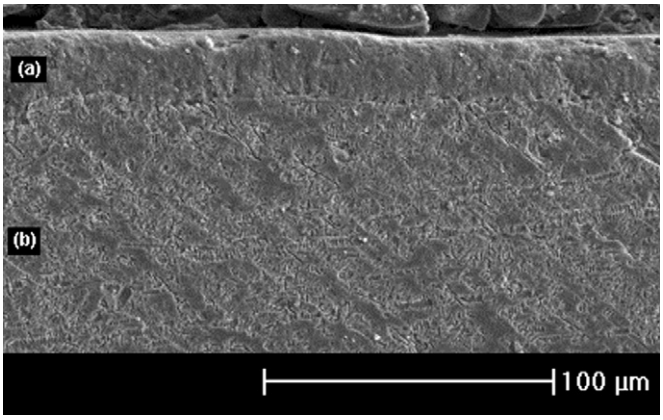

Fig. 5. SEM observation of a glass monolith heat treated at 775 °C/30 min showing (a) the crystalline growing from the surface and (b) bulk of the material.

by Montedo et al. [2]. For example, Fig. 5 obtained from a monolith heat treated at 775 °C/30 min shows a crystalline layer growing from the surface toward to the bulk of the material. A formed layer with 25 μm thickness was obtained for a threshold time of 30 min at 775 °C.

3.4. Sintering behavior

Fig. 6 shows a plot of the linear shrinkage ($\Delta l/l_o$) *vs.* the sintering temperature, *T,* for the investigated LZSA glass ceramic.

According to Fig. 6, sintering has started at about 590 °C, which is in very good agreement with T_g obtained in the beam-bending test (Fig. 2) and by DTA (Fig. 3). Taking into account the first derivative of the $\Delta l/l_o$-*T* plot, the maximum shrinkage rate was found to be at 690 °C (Fig. 6) whilst at 790 °C the shrinkage rate was almost zero. Higher sintering rates were inhibited probably due to the beginning of the crystallization process. This seems to have begun at about 680 °C (Fig. 3). All the reported temperatures are in good agreement with the thermal events recorded in the DTA scan from Fig. 3. The values of $\Delta l/l_o$ apparently did not change during the crystallization interval. The sample initiated the expansion process at about 920 °C before complete melting at above 1050 °C.

From Fig. 6, four threshold temperatures were chosen to assess the best heat treatment conditions for the obtainment of denser materials. For each temperature, a 60 min swelling time was applied, except for the last temperature (1050 °C) at which a swelling time of 180 min was applied. The criteria involved in the choice are detailed as follows:

a) 685 °C as the temperature barely under that of the maximum shrinkage rate, assuming that the crystallization rate is still low at this temperature;
b) 800 °C as the temperature at which the shrinkage rate was almost zero due to increasing crystallization rates;
c) 900 °C as the temperature of the end of the crystallization interval and,
d) 1020 °C as the temperature used to verify the behavior of the investigated glass ceramic regarding to the $\Delta l/l_o$ and the microstructure, at a very high temperature.

Fig. 7 shows the plot $\Delta l/l_o$- time, *t,* for each investigated temperature. At 685 °C, the 60 min swelling time has increased the $\Delta l/l_o$ from 10 to 21%. In fact, Fig. 8 shows that 60 min swelling time at 685 °C significantly reduced the porosity in the microstructure.

At 800 °C, however, the maximum $\Delta l/l_o$ (22%) was achieved with 5 min swelling time. Although the crystallization has already begun at 800 °C, the shrinkage intensity apparently did not interfere with the sintering. According to Montedo et al. [4], this behavior can be associated with some retarded crystalline phase formation at this temperature, for instance due to the formation of $ZrSiO_4$. This phase is used to crystallize in the bulk of the glassy phase and not on the free surfaces. Actually, the microstructure of the samples kept for 10 min at 800 °C (Fig. 9) was denser than that of those kept for 60 min at

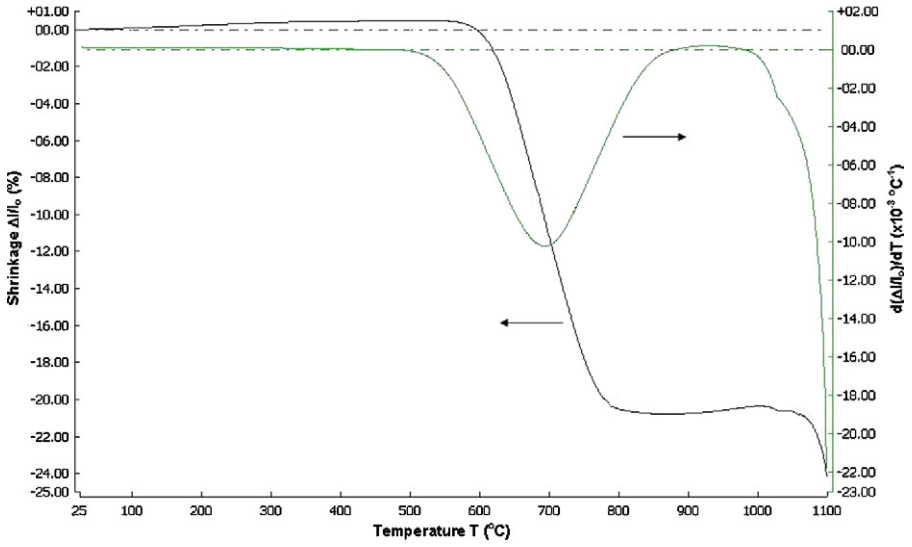

Fig. 6. Shrinkage-temperature plot.

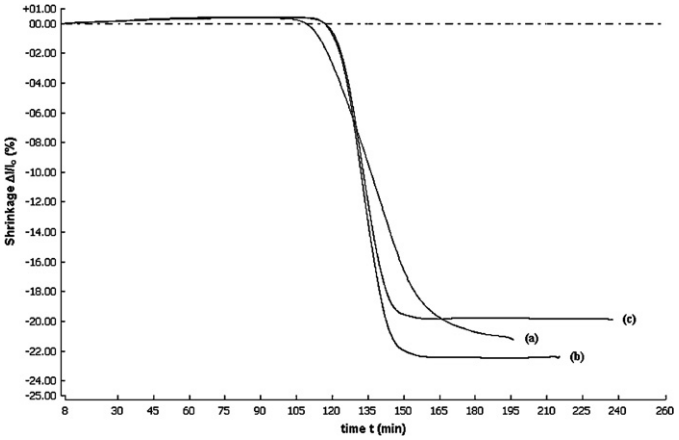

Fig. 7. Plot of $\Delta l/l_o$ *vs.* time of the investigated composition at: (a) 685 °C, (b) 800 °C and (c) 900 °C.

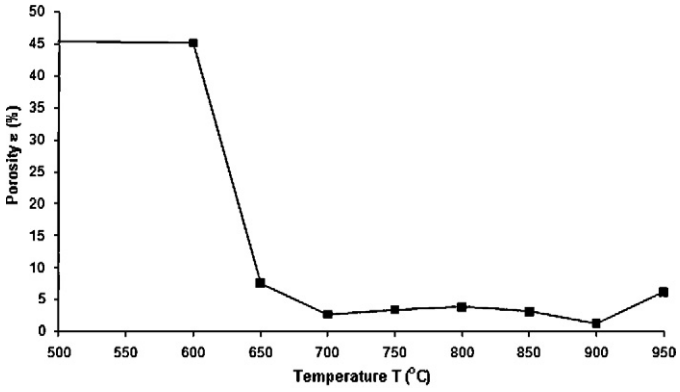

Fig. 10. Porosity *vs.* temperature of the investigated composition.

685 °C. Fig. 9 also shows that the resulting microstructure of samples kept for 60 min at 800 °C is basically the same as the microstructure of samples kept for 10 min at the same temperature. In this case, it can be shown that longer threshold times would not lead to an evolution of the final microstructure, but to higher energy consumptions. This phenomenon is also evidenced in Fig. 10. Up to temperatures of 700 °C the material will continuously densify. From 700 °C on, almost no further densification of the glass ceramic can be observed.

On the other hand, the maximum $\Delta l/l_o$ (20%) at 900 °C was achieved instantly, i.e. a swelling time at 900 °C would not increase the shrinkage. Additionally, Fig. 11 shows that no significant differences between the microstructures obtained without and with the 60 min swelling time (Fig. 11a and b, respectively) can be observed.

Comparing the microstructure obtained at 800 °C/10 min ($\Delta l/l_o$ = 22%), Fig. 11a, with that obtained at 1020 °C/180 min ($\Delta l/l_o$ = 15%) from Montedo et al. [4], Fig. 12, it is possible to notice that a continuous heating of the investigated composition up to higher temperatures would not lead to a low porosity glass ceramic product. A swelling time of 60 min at 685 °C or of 10 min at 800 °C would be enough for the material to achieve a full densification before the crystallization process starts. According to Montedo et al. [4], β-spodumene$_{ss}$ and $ZrSiO_4$ crystallize at 800 and 850 °C, respectively. The strong reduction of the shrinkage rate at temperatures of 800 °C up

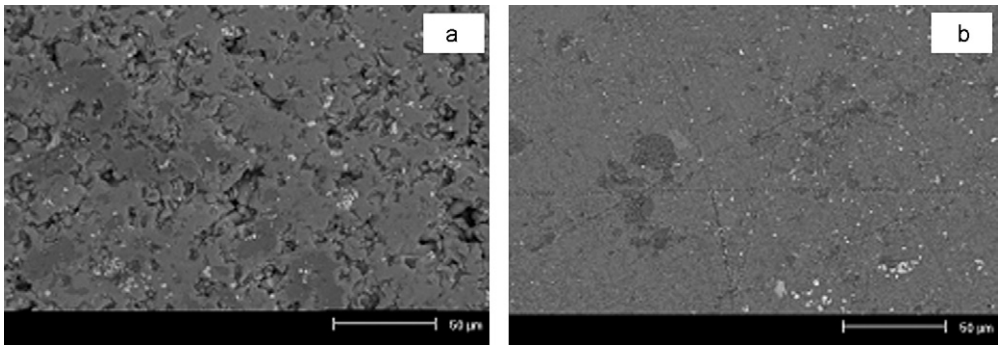

Fig. 8. SEM observations of the microstructure samples heat treated at 685 °C: (a) no swelling time and (b) 60 min swelling time.

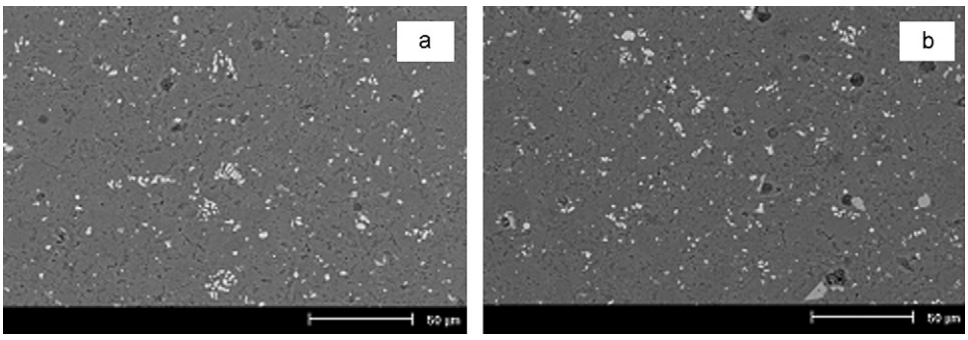

Fig. 9. SEM observations of the microstructure samples heat treated at 800 °C for: (a) 10 min and (b) 60 min.

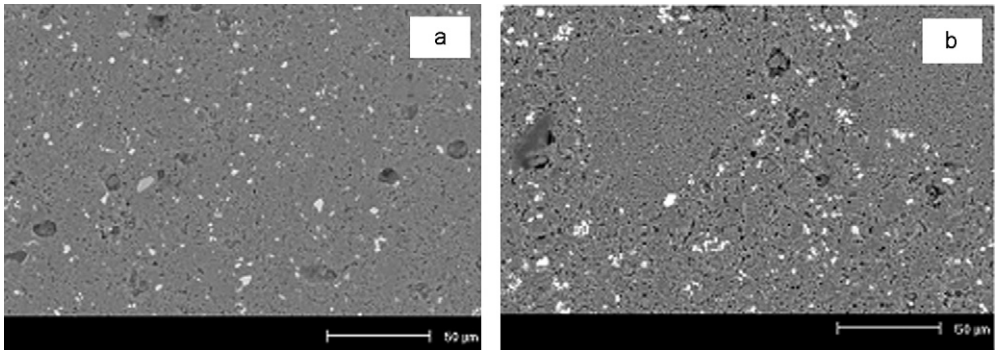

Fig. 11. SEM observations of the microstructure samples heat treated at 900 °C: (a) no swelling time and (b) for 60 min swelling time.

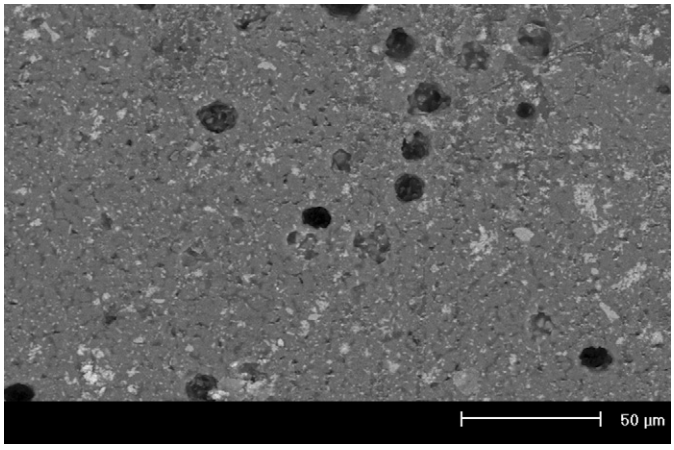

Fig. 12. SEM observation of the microstructure samples heat treated at 1020 °C for 180 min.

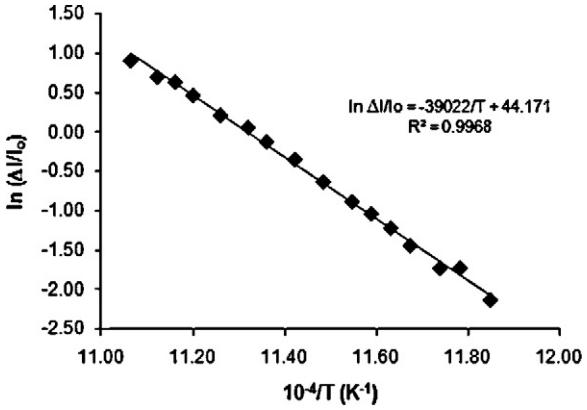

Fig. 13. Plot of ln ($\Delta l/l_o$) *vs.* $1/T$ for initial-stage CRH sintering of the LZSA composition.

to 920 °C is an evidence of the beginning of some crystallization. This effect becomes more evident at temperatures higher than 800 °C, when the β-spodumene$_{ss}$ starts the crystallization at the surface, increasing the viscosity of the residual glassy phase around the particles and reducing the densification rates.

Considering the maximum values of $\Delta l/l_o$, the evolution of the microstructures and the investigated heat-treatment conditions, the highest densification was obtained in samples submitted to a heating rate of 5 °C.min^{-1}, with 10 min swelling time at 800 °C. This means that if the final objective is obtaining highly dense glass ceramics, the material should be heat treated in these conditions before a threshold temperature for crystallization is reached.

3.5. Sintering kinetics

The activation energy for the initial stage of sintering was defined by the shrinkage plot according to Young and Cutler [17]. Fig. 13 shows the plot of ln ($\Delta l/l_o$) *vs.* $1/T$ using the data related to the beginning of sintering (580–630 °C). The obtained data present a low scatter along the analyzed temperature interval. As predicted by Woolfrey and Bannister [9], the slope of the straight line is directly $-Q/(n+1)R$. However, considering $n = 0$ for viscous flow sintering, Woolfrey and Bannister [9], a Q value of 314 kJ.mol^{-1} is obtained. Cutler [10] found values between 356 and 377 kJ.mol^{-1} for the sintering activation energy of soda-lime glass spheres with diameters in the 15-25 μm range whilst Shilo et al. [18] found values of 138 and 120 kJ.mol^{-1}, respectively, for lead glass and silicate glass spheres (no information about de sphere dimensions has been provided).

On the other hand, applying the Dorn method to the temperatures in the sintering range ($V_1 = 0.26$ min^{-1} for $T_1 = 868.5$ K and $V_2 = 0.77$ min^{-1} for $T_2 = 890.5$ K), the value of the activation energy for sintering in the LZSA composition investigated is 314 kJ.mol^{-1}. The excellent agreement between the values of activation energy for sintering given in the plot of ln ($\Delta l/l_o$) *vs.* $1/T$ and by applying the Dorn method support the initial hypothesis of sintering by viscous flow at the beginning of the process, i.e. $n = 0$, indicating also the accuracy of the experimental results obtained by dilatometry measurements.

4. Conclusions

Dilatometry measurements were carried out to describe the kinetics of the initial sintering stage for a 18.8Li_2O 8.3ZrO_2 64.2SiO_2 8.7Al_2O_3 glass ceramic composition at a constant heating rate with a view to optimizing the densification process of this material. The activation energy obtained by dilatometry measurements for sintering of this system was 314 kJ.mol^{-1}, which is in excellent agreement with the value calculated by the Dorn method. The best heat treatment parameters for sintering

were found to be a 5 °C.min^{-1} heating rate with a 10 min swelling time at 800 °C. At optimized conditions, 22% of linear shrinkage was achieved with a porosity of 3.5%. SEM observations confirmed that the highest densification were obtained for samples sintered at 800 °C/10 min, indicating a high application potential of the investigated glass ceramic composition for LTCC technologies. Complementary investigations concerning the mechanical, electrical and thermal properties of this system are ongoing.

Acknowledgements

The authors are grateful to the Brazilian Foundation for the Coordination of Higher Education Graduate Training (CAPES) and to the National Council of Scientific Technological Development (CNPq) for supporting this work. Moreover, the authors are also very thankful to Prof. Peter Greil at the Department of Glass and Ceramics, University of Erlangen-Nuremberg, for supporting some of the laboratorial tests necessary to the development of this work.

References

[1] Montedo, O.R.K., Oliveira, A.P.N. de, Klein, A.N., 2001. Design, characterization and preparation of glass-ceramic glazes belonging to the LZSA glass system. In: Third International Latin-American Conference on Powder Technology, Florianópolis, Brazil, pp.124-132.

[2] O.R.K. Montedo, F.M. Bertan, R. Piccoli, D. Hotza, A.N. Klein, A.P.N. de Oliveira, Low thermal expansion sintered LZSA glass-ceramics, Am. Ceram. Soc. Bull. 87 (2008) 34–47.

[3] C.M. Gomes, A.P.N.de Oliveira, D. Hotza, N. Travitzky, P. Greil, LZSA glass-ceramic laminates: Fabrication and mechanical properties, J. Mat. Proc. Techn. 206 (2008) 194–201.

[4] O.R.K. Montedo, F.J. Floriano, J.de Oliveira Filho, E. Angioleto, A.M. Bernardin, Sintering behavior of LZSA glass-ceramics, Materials Research. 12 (2) (2009) 197–200.

[5] J. Frenkel, Viscous Flow of crystalline bodies under the action of surface tension, J. Phys. 9 (5) (1945) 385–391.

[6] W.D. Kingery, M. Berg, Study of initial stages of sintering solids by viscous flow, evaporation-condensation and self-difusion, J. Appl. Phys. 26 (10) (1955) 1205–1212.

[7] G.W. Scherer, Sintering of low-density glasses: Part 1. Theory, J. Am. Ceram. Soc. 60 (1977) 239–243.

[8] K.D. Kim, T.K. Khalil, Sintering behaviour of gel powder in binary glass-forming SiO_2-TiO_2 system, J. Non-Cryst. Solids. 195 (1996) 218–222.

[9] J.L. Woolfrey, M.J. Bannister, Nonisothermal techniques for studying initial-stage sintering, J. Am. Ceram. Soc 55 (8) (1972) 390–394.

[10] I.B. Cutler, Sintering of glass powders during constant rates of heating, J. Am. Ceram. Soc. 52 (1) (1969) 14–17.

[11] W.S. Young, S.T. Rasmussen, I.B. Cutler, in: Ultrafine-Grain, Ceramics, J.J. Burke, N.L. Reed, V. Weiss (Eds.), Determination of an effective viscosity of powders as a function of temperature., Syracuse University Press, Syracuse, New York, 1970, pp. 185–202.

[12] J.J. Bacmann, G. Cizeron, Dorn method in the study of initial phase of uranium dioxide sintering, J. Am. Ceram. Soc. 51 (4) (1968) 209–212.

[13] T.K. Khalil, A.R. Boccaccini, Heating microscopy study of the sintering behaviour of glass powder compacts in the binary system SiO_2-TiO_2, Materials Letters. 56 (2002) 317–321.

[14] R.W. Rice, Porosity of Ceramics, Marcel Dekker, Inc, New York, 1998, 43-92.

[15] A.R. Boccaccini, Z. Fan, A new approach for the Young's modulus porosity correlation of ceramic materials, Ceram. Int. 23 (1997) 239–245.

[16] J.J. Shyu, H.H. Lee, Sintering, crystallization, and properties of B_2O_3/P_2O_5 dopped of Li_2O Al_2O_3. $4SiO_2$ glass-ceramics, J. Am. Ceram. Soc. 78 (8) (1995) 2161–2167.

[17] W.S. Young, I.B. Cutler, Initial sintering with constants rates of heating, J. Am. Ceram. Soc. 53 (12) (1970) 659–663.

[18] A.E. Shilo, E.K. Bondarev, S.A. Kukharenko, Sintering of low-melting glass powders and glass-abrasive composites, Science of Sintering 35 (2003) 117–124.